

1 **Photoacoustic measurement with infrared band-pass filters significantly overestimate**

2 **NH<sub>3</sub> emissions from cattle houses due to VOCs interferences**

3

4

5 Dezhao Liu<sup>1,2\*</sup>, Li Rong<sup>2</sup>, Jesper Kamp<sup>2</sup>, Xianwang Kong<sup>1</sup>, Anders Peter S. Adamsen<sup>3</sup>,

6 Albarune Chowdhury<sup>2</sup>, Anders Feilberg<sup>2\*</sup>

7

8 1- Zhejiang University, College of Biosystems Engineering and Food Science, Yuhangtang

9 Road 866, 310058 Hangzhou, China

10 2- Aarhus University, Department of Engineering, Finlandsgade 22, 8200 Aarhus N, Denmark

11 3- APSA, c/o Agro Business Park, Niels Pedersens Allé 2, DK-8830 Tjele, Denmark

12

13 **Corresponding author: Dezhao Liu: [dezhaoliu@zju.edu.cn](mailto:dezhaoliu@zju.edu.cn);**

14 **Anders Feilberg: [af@eng.au.dk](mailto:af@eng.au.dk)**

15

16

17

18

19

20

21

22

23 **Abstract:** Infrared photoacoustic spectroscopy using band-pass filters (PAS) is a widely used  
24 method for measurement of NH<sub>3</sub> and greenhouse gas emissions (CH<sub>4</sub>, N<sub>2</sub>O and CO<sub>2</sub>) especially  
25 in agriculture, but non-targeted gases such as volatile organic compounds (VOCs) from cattle  
26 barns may interfere with target gases causing inaccurate results. This study made an estimation  
27 of NH<sub>3</sub> interference in PAS caused by selected non-targeted VOCs which were simultaneously  
28 measured by a PAS and a PTR-MS (proton transfer reaction mass spectrometry). Laboratory  
29 calibrations were performed for NH<sub>3</sub> measurement and VOCs were selected based on a  
30 headspace test of the feeding material (maize silage). Strong interferences of VOCs were  
31 observed on NH<sub>3</sub> and greenhouse emissions measured by PAS. Particularly, ethanol, methanol,  
32 1-butanol, 1-propanol and acetic acid were found to have the highest interferences on NH<sub>3</sub>,  
33 giving empirical relationships in the range of 0.7 to 3.3 ppmv NH<sub>3</sub> per ppmv VOC. A linear  
34 response was typically obtained, except for a non-linear relation for VOCs on N<sub>2</sub>O  
35 concentration. The corrected online NH<sub>3</sub> concentrations measured by PAS in a dairy farm (with  
36 empirical relationships  $2.1 \pm 0.8$  and  $2.9 \pm 1.9$  for Location One and Location Two, respectively)  
37 were confirmed to be correlated ( $R^2 = 0.73$  and  $0.79$ ) to the NH<sub>3</sub> concentration measured  
38 simultaneously by the PTR-MS, when the empirical corrections obtained from single VOC tests  
39 were applied.

## 40 **1 Introduction**

41 Measurements of ammonia and greenhouse gas (CH<sub>4</sub>, N<sub>2</sub>O and CO<sub>2</sub>) emissions are gaining  
42 increasing attention due to stronger interests on global change and air pollution. Ammonia not  
43 only causes serious environmental problems such as soil acidification and pollution of  
44 underground water and surface water (van Breemen et al., 1983; Pearson and Stewart, 1993;

45 Erisman et al., 2007), but is also important for fine particle formation (Bouwman et al., 1997;  
46 Seinfeld and Pandis, 1997; Pinder et al., 2007). Greenhouse gas emissions, on the other hand,  
47 are causing climate change (Thomas et al., 2004; Chadwick et al., 2011). Livestock husbandry  
48 was estimated to be responsible for more than 80 % of the ammonia emission in Western Europe  
49 (Hutchings et al., 2001; EMEP, 2013) and more than 60% in China (Paulot et al., 2014). In the  
50 U.S.A, agriculture accounts for ~90 % of the total ammonia emissions (Aneja et al., 2009).  
51 Meanwhile, agriculture accounts for 52 and 84 % of global anthropogenic methane and nitrous  
52 oxide emissions (Smith et al., 2008). Accurate measurements of ammonia and greenhouse  
53 emissions are therefore vital for reliable emission estimation and thereby the possible reduction  
54 of these emissions through various efforts, such as air cleaning with biotrickling filters and air  
55 scrubbers (Melse and Van der werf, 2005; De Vries and Melse, 2017). For ammonia  
56 measurements, more than 30% difference between different methods has been reported  
57 (Scholtens et al., 2004).

58 Infrared photoacoustic spectroscopy (PAS) is a widely-used technique for studies of air  
59 emissions especially within agriculture (Osada et al., 1998; Osada and Fukumoto, 2001;  
60 Emmenegger et al., 2004; Schilt et al., 2004; Heber et al., 2006; Elia et al., 2006; Blanes-Vidal  
61 et al., 2007; Hassouna et al., 2008; Rong et al., 2009; Ngwabie et al., 2011; Cortus et al., 2012;  
62 Joo et al., 2013; Wang-Li et al., 2013; Iqbal et al., 2013; Zhao et al., 2016; Ni et al., 2017; Lin  
63 et al., 2017). The PAS technique determines the gas concentrations through measuring acoustic  
64 signals caused by cell pressure changes when gas absorbs energy from infrared light at a  
65 specific wavelength range using an optical filter and a chopper (Iqbal et al., 2013). For example,  
66 the Innova 1312 and later versions (Lumasense Technologies, Ballerup, Denmark) uses the PAS

67 principle and was previously verified by the US EPA and recommended by the Air Resources  
68 Board in California (CARB, 2000). In principle, this instrument "is capable of measuring  
69 almost any gas that absorbs infrared light" (Innova, Lumasense Technology A/S, Denmark).  
70 The method is based on nondispersive broadband spectroscopy and selectivity is achieved by  
71 using appropriate wavelength filter, with one filter for each targeted trace gas. Innova 1312 and  
72 1412 instruments have been used in a large number of tests to measure NH<sub>3</sub>, CH<sub>4</sub>, CO<sub>2</sub> and N<sub>2</sub>O  
73 for agricultural applications. Water vapor is also measured to account for the strong absorption  
74 of water throughout the infrared spectrum (Christensen, 1990a). Nevertheless, since the infrared  
75 spectroscopic method is applied for measuring gas concentrations in PAS, the overlapping of  
76 IR spectra with non-targeted gases can introduce significant interferences due to the absorption  
77 of infrared light at similar wavelengths. The specificity is limited by the bandwidth of the  
78 optical filters. The interferences can be corrected by the instrument software through cross-  
79 compensation for all target gases when the instrument is calibrated (Christensen, 1990a;  
80 Lumasense, 2012), but understanding and estimation of interferences from non-targeted gases  
81 needs to be considered in each specific measurement situation. This is especially important for  
82 agricultural applications where the manure and the animal feed may emit various types of gases  
83 depending on the management and operations in the animal houses (Hassouna et al., 2013;  
84 Moset et al., 2012). Therefore, two key questions exist: (a) what is the magnitude of  
85 interferences that can be expected in agricultural environments, and (b) is it possible to quantify  
86 and correct interferences in a reasonable way? Until now, the PAS interference has not been  
87 well estimated and corrected for, although interferences were previously suspected in livestock  
88 facilities (Phillips et al., 2001; Mathot et al., 2007; Ni & Heber, 2008). Flechard et al. (2005)

89 suspected that the N<sub>2</sub>O concentration from soil measured by PAS (Innova 1312) was heavily  
90 influenced by CO<sub>2</sub> and temperature even when cross-interference compensation was applied;  
91 they developed an alternative correction algorithm based on controlled N<sub>2</sub>O/CO<sub>2</sub>/H<sub>2</sub>O ratios  
92 under selected temperature. Zhao et al (2012) claimed that the internal cross compensation  
93 could eliminate the interferences between target gases, and quantified interferences of non-  
94 targeted gas of NH<sub>3</sub> on targeted gases of ethanol, methanol, N<sub>2</sub>O, CO<sub>2</sub>, and CH<sub>4</sub>, however,  
95 without giving specific relationships. Iqbal et al. (2013) also demonstrated that a careful  
96 calibration could eliminate the internal cross interferences of high water vapor and CO<sub>2</sub>  
97 concentrations on low concentrations of N<sub>2</sub>O at the soil surface by comparison to GC  
98 measurements. Nevertheless, tests of interferences by non-targeted VOCs were not included in  
99 their study, likely due to the typical low concentrations of VOC in soil (Insam and Seewald,  
100 2010). Hassouna et al. (2013) presented a field study on dairy cow buildings, where  
101 interferences on NH<sub>3</sub>, CH<sub>4</sub> and N<sub>2</sub>O were observed. The interferences were suspected to be  
102 caused by VOCs (acetic acid, ethanol and 1-propanol) that they measured simultaneously. In  
103 their study, two PAS instruments were applied with one of them allocated with optical filters of  
104 these VOCs (NH<sub>3</sub> optical filter was included for both PAS). Still, no empirical relationships  
105 were given in terms of tested volatile organic compounds, which were typically emitted from  
106 feeding materials such as maize silage (Howard et al., 2010; Malkina et al., 2011). The  
107 correction of interferences of non-targeted VOCs on NH<sub>3</sub> emission is also essential for the  
108 evaluation of emission abatement technologies such as air scrubbers, especially when the inlet  
109 VOC concentrations are relatively high. An overestimation of ammonia removal efficiency  
110 could easily be obtained since less interference would be expected for the outlet VOCs

111 especially for water-soluble compounds such as the VOCs investigated in this study.  
112 In this work, an evaluation of interferences by non-targeted VOCs on targeted NH<sub>3</sub> and  
113 greenhouse gas measurements by PAS is presented. The interference on NH<sub>3</sub> was tested by  
114 simultaneous application of Proton-transfer-reaction mass spectrometry (PTR-MS), Cavity  
115 Ring-Down Spectroscopy (CRDS) and PAS. The experiments were as follows: (1) ammonia  
116 laboratory calibration by PAS, PTR-MS and CRDS; (2) VOC selection for testing of  
117 interference on ammonia measured by PAS; (3) Effect of VOCs on ammonia and greenhouse  
118 emissions measured by the PAS; (4) Field confirmation of interferences of non-targeted VOCs  
119 on ammonia measurement and test of potential for data correction.

## 120 **2 Materials and methods**

### 121 **2.1 Instrumentation for gas concentrations measurement**

122 In this study, a PTR-MS, a CRDS NH<sub>3</sub> analyzer and a PAS gas analyzer were used to measure  
123 trace gas concentrations in air. PTR-MS is a state-of-the-art and widely used technique for  
124 highly sensitive online measurements of VOCs (De Gouw and Warneke, 2007; Blake et al.,  
125 2009; Yuan et al., 2017). PTR-MS can also measure a few inorganic compounds such as  
126 ammonia (at m/z 18) since the proton affinity (204.0 kcal/mol) of ammonia is higher than that  
127 of water (165.0 kcal/mol). Since the intrinsic ion at m/z 18 is always formed in the plasma ion  
128 source (Norman et al., 2007), ammonia measurements by PTR-MS are routinely corrected for  
129 instrumental background contribution. The typical m/z 18 background signal corresponds to a  
130 few hundred ppbv of NH<sub>3</sub>. The background signal is relatively stable and still allows for NH<sub>3</sub>  
131 detection limits of 20-50 ppb. For agricultural measurement conditions, concentrations are  
132 typically from a few hundred ppb to >10 ppm (e.g., Rong et al., 2009). When total gas

133 concentration measured by PTR-MS is higher than approximately 10 ppmv, dilution is needed  
134 to keep the primary ion signals stable. A high-sensitivity PTR-MS (Ionicon Analytik GmbH,  
135 Innsbruck, Austria) was applied for the test of ammonia calibration in the laboratory, effects of  
136 non-targeted VOCs on ammonia measurement and field confirmation of interferences of non-  
137 targeted VOCs on ammonia measurement. Standard conditions with a total voltage of 600 V in  
138 the drift tube were utilized for the PTR-MS. Pressure and temperature in the drift tube were  
139 maintained in the range of 2.1-2.2 mbar and at 60 °C, respectively, which gives an E/N ratio of  
140 ca. 135 Townsend. The inlet of the PTR-MS is PEEK tubing of 1.2 m length with 0.64 mm  
141 inner diameter (ID) and 1.6 mm outer diameter (OD). The inlet flow to the PTR-MS during  
142 calibration test and measurements was kept ~150 mL/min. The inlet temperature was  
143 maintained at 60 °C. The instrument calibration was performed based on specific reaction rate  
144 constants and mass discrimination factors (accuracy better than 12%), as described in our  
145 previous study (Liu et al., 2018). Mass calibration was performed before each test, while mass  
146 discrimination calibration was performed for every two weeks.

147 CRDS determines the gas concentration (e.g., NH<sub>3</sub>) by measuring the ring-down time of light  
148 in the cavity due to absorption by a targeted gas species, which is compared to the ring-down  
149 time without any additional absorption due to a targeted gas species. The light source is a laser  
150 with tunable wavelength (von Bobruzki et al., 2010; Picarro, 2017). The very long effective  
151 path length of the light in the cavity (e.g., over 20 km for 25 cm cavity) (Picarro, 2017), enables  
152 a significantly higher sensitivity compared to conventional absorption spectroscopy (Berden et  
153 al., 2000; von Bobruzki et al., 2010). There is negligible interference from VOCs on CRDS  
154 measurements, which makes CRDS ideal to measure NH<sub>3</sub> concentrations in this setting (Kamp

155 et al., 2019). A G2103 Analyzer (Picarro Inc., Sunnyvale, CA, USA) using CRDS technique  
156 was applied in this study for the test of ammonia laboratory calibration and the effect of non-  
157 targeted VOCs on ammonia measurement. The accuracy of the CRDS instrument is routinely  
158 checked against a certified reference gas as described by Kamp et al (2019). The CRDS analyzer  
159 was equipped with two in-line, sub-micron polytetrafluoroethylene (PTFE) particulate matter  
160 filters; one at the gas inlet at the back of the analyzer and one at the inlet of the cavity to protect  
161 the highly reflective mirrors. The inlet of the CRDS is a PTFE (PTFE) tubing of 1.5 m length  
162 with 6.4 mm outer diameter. The optical cavities incorporate precise temperature ( $\pm 0.005$  °C)  
163 and pressure ( $\pm 0.0002$  atm) control systems. In this study, both the temperature and pressure  
164 of the air sample continuously flowing through the optical cavity are tightly controlled at all  
165 times to constant values of 45 °C and 140 Torr, respectively. The measurement interval is  
166 around 2 seconds. The CRDS analyzer measured the water vapor simultaneously.

167 A photoacoustic multi-gas monitor 1312 (Innova, Lumasense Technology A/S, Denmark) was  
168 compared with the PTR-MS and the CRDS for ammonia calibration and non-targeted VOCs  
169 on ammonia measurement. An infra-red-light source was used for the PAS instrument and the  
170 principle for the measurement is as follows. The infrared radiation can interact with a molecule  
171 and transfer energy to it if the frequency of the radiation is the same as the frequency of  
172 vibration within the molecule. When the molecule absorbs IR light, it vibrates with greater  
173 amplitude. This increased activity is short-lived, however, and the excited molecule very  
174 quickly transfers its extra energy to other molecules in the vicinity by collision. The increased  
175 kinetic energy leads to an increase in the measurement chamber temperature and pressure. A  
176 microphone is used to detect the consequently fluctuating pressure. The sample integration time



177 to measure ammonia by PAS was 20 s. The instrument used 6 optical filters for NH<sub>3</sub>, CH<sub>4</sub>, CO<sub>2</sub>,  
178 H<sub>2</sub>O, N<sub>2</sub>O and SF<sub>6</sub>. The specifications of the optical filters are shown in Table S1. Water vapor  
179 must be included for PAS measurement since the absorbance spectrum of water overlap with  
180 other gases such as N<sub>2</sub>O and CO<sub>2</sub> thus causing interferences. According to the manufacturer,  
181 the Innova 1312 has linear response over a wide dynamic range, with the possibility to make  
182 self-calibration (Lumasense, 2012). Before the measurements presented in this study, the  
183 supplier calibrated the instrument. During the study the instrument was calibrated based on a  
184 certified gas cylinder containing 99.7 (± 10 %) ppmv ammonia (AGA A/S, Copenhagen,  
185 Denmark). The interferences between the target gases were therefore supposed to be eliminated  
186 through internal cross compensation (Christensen, 1990b; Zhao et al., 2012).

## 187 **2.2 Experiment 1: laboratory test on ammonia calibration**

188 Instrumental background signals, ammonia calibrations and instrumental response times were  
189 characterized for the PAS, PTR-MS and CRDS instruments. For the background measurement,  
190 zero air controlled by a mass flow controller (Bronkhorst, Ruurlo, The Netherlands) was  
191 supplied, and measurement was performed individually for each instrument. The zero air was  
192 supplied from a HiQ zero air station (Linde AG, Munich, Germany). The selected ion  
193 measurement mode was used for the PTR-MS with m/z 18 being used for ammonia detection.  
194 For the calibration test, a factory-calibrated gas cylinder (AGA A/S, Copenhagen, Denmark)  
195 containing 99.7 (± 10 %) ppmv ammonia was used. Mass flow controllers (Bronkhorst, Ruurlo,  
196 The Netherlands) were used to dilute the gas from the cylinder with zero air to achieve the  
197 desired NH<sub>3</sub> concentration levels (0-11 ppmv). For the test of response decay time, zero air flow  
198 was supplied to the instruments at first, then switched to a diluted flow (via 2-levels of mass

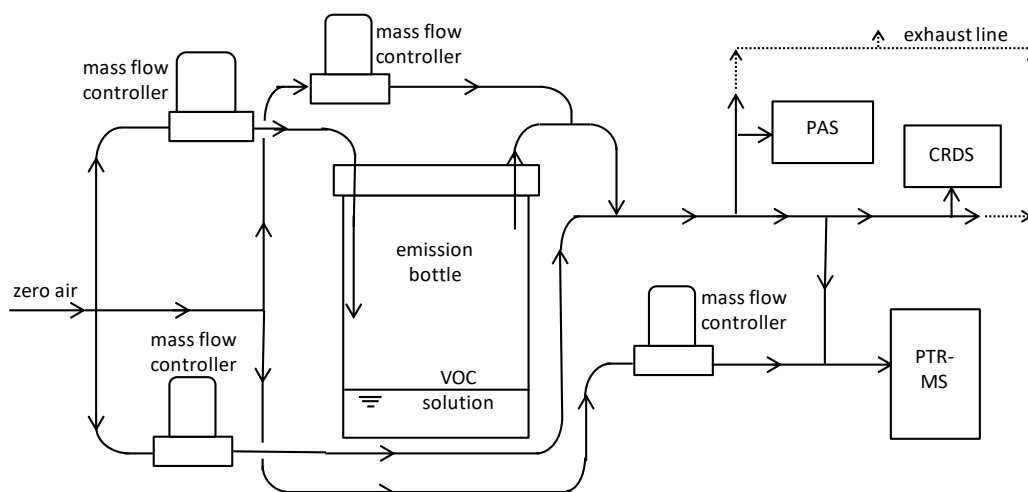
199 flow controllers) with ammonia concentration around 5.2 ppmv supplied to all three  
200 instruments simultaneously. Subsequently, the ammonia supply was set to zero to test the decay  
201 time. Four individual decay time tests were performed for the PAS, to confirm the long decay  
202 time of the instrument with low ammonia concentrations (5.2-8.8 ppmv) or high ammonia  
203 concentration (99.7 ppmv). For the test of response time for the PAS, two different levels of  
204 ammonia concentration were introduced individually to the instrument, to test the dependence  
205 of the response time on ammonia concentration.

### 206 **2.3 Experiment 2: VOCs selection test**

207 A headspace test was performed and VOCs were selected through a PTR-MS measurement as  
208 preparation to the interference tests of VOCs on ammonia measured by the PAS. Maize silage  
209 is typical feeding material to the cows and silage is generally considered an important source  
210 of gaseous VOC in cattle barns. A sample of maize silage was collected from the farm where  
211 the field experiment was performed (Skjern, Jutland, Denmark, altitude: 55°59'36.6", longitude:  
212 8°29'53.52"). The silage was then transferred to the laboratory immediately for the headspace  
213 test. A clean PTFE container (58×38×43 cm) with two oval holding holes (6×8 cm) on the  
214 sides was used for the headspace test. The container was partly open and the silage filled half  
215 of the container. A 1-meter 1/4-inch OD PTFE tube was used for the test, with one end placed  
216 around 5 cm above the silage, and the other side connected to a T-piece. One side of the T-piece  
217 was connected to a 1/8-inch OD PTFE tube (around a half meter) which was connected to the  
218 inlet of the PTR-MS. The flow rate of the PTR-MS was kept at 150 mL/min. A zero-air dilution  
219 flow (75 mL/min) was supplied to the T-piece to make 1:1 dilution to keep the total  
220 concentration below 10 ppmv. The headspace measurement was performed by the PTR-MS in

221 scan mode, and masses were measured from  $m/z$  21 to  $m/z$  250 with 200 ms for each mass. The  
 222 selection of VOCs was based on the scan results and relevant literature data on silage VOC,  
 223 with the following VOCs being selected: ethanol, methanol, acetaldehyde, acetic acid, 2-  
 224 butanone, acetone, 1-propanol and 1-butanol (Howard et al., 2010; Malkina et al., 2011; Hafner  
 225 et al., 2013). These 8 selected VOCs were tested for empirical relationships ( $C_{NH_3obs}/C_{VOC}$ ) with  
 226 respect to contribution to measured  $NH_3$  concentration ( $C_{NH_3obs}$ ). All chemicals were purchased  
 227 from Sigma-Aldrich with at least analytical grade purity.

228



229

230 **Figure 1.** A diagram of the experimental set-up for test of ammonia interference due to VOC.

### 231 2.4 Experiment 3: Laboratory test for empirical relationships

232 The diagram of the setup for the laboratory calibration test is shown in Figure 1. In the setup, a  
 233 water solution containing the single VOC was purged from the headspace by dry and clean air  
 234 (or nitrogen for one test on methanol), with flow controlled by a mass flow controller. The air  
 235 or nitrogen was supplied through a charcoal/silica gel filter. One-liter airtight glass bottles were  
 236 used for the water solution containing the VOC, and 1/4-inch OD PTFE tube was used in the  
 237 setup. The purged air flow was diluted with air through a two-step dilution. The flows were

238 adjusted according to the purged VOC concentration and the desired final VOC concentration.  
239 The water solution was prepared by using a volume ratio of VOC:Water of 1:5, with purging  
240 by clean air controlled by 2 mass flow controllers in order to reach a desired concentration  
241 range. For the laboratory test, the diluted air containing VOC was connected to the PAS, the  
242 CRDS and the PTR-MS for simultaneous measurements. The overall flow was maintained at a  
243 level above the total maximum sampling flow of all three instruments and excess flow was  
244 vented through a T-piece. For the PTR-MS measurement, a further dilution by zero air was  
245 typically used to keep the total VOC concentrations below 10 ppmv to avoid depletion of the  
246 primary ion,  $\text{H}_3\text{O}^+$ . Selected ion measurement mode was applied for the PTR-MS, with an  
247 integration time of 2 seconds for the tested VOC mass. During the experiments, the humidity  
248 was kept relatively low and stable, with dry clean air used for dilution for all cases, except for  
249 one test on methanol, which was also tested under nitrogen condition.

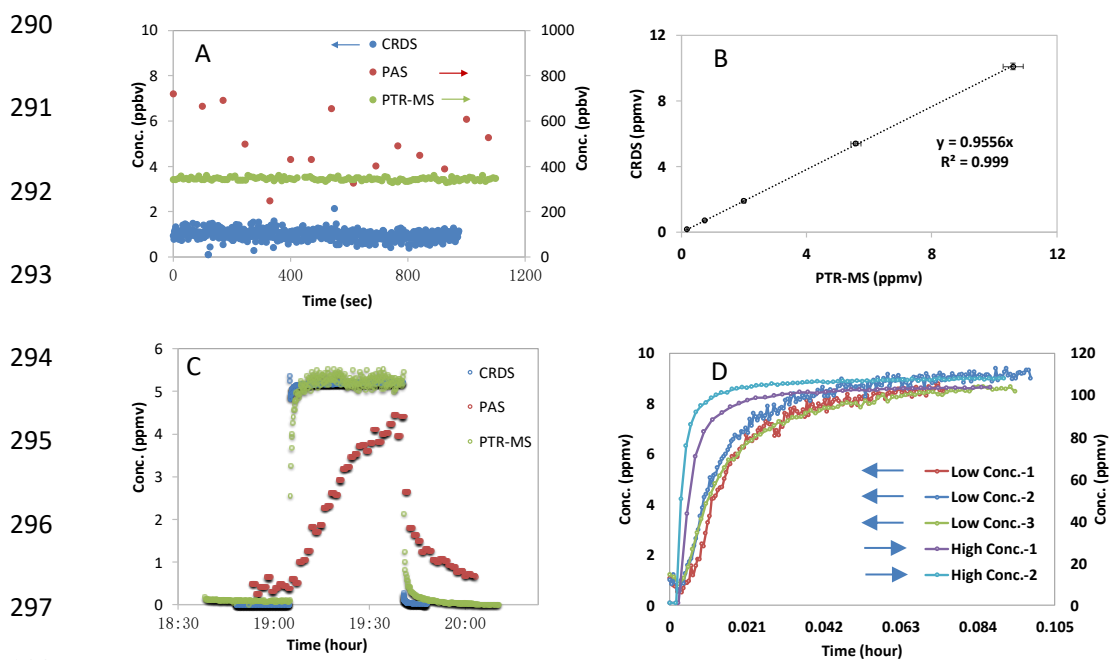
## 250 **2.5 Experiment 4: Field test for validation of empirical relationships**

251 The field demonstration test for non-targeted VOCs on ammonia measurement by the PAS was  
252 performed in the dairy farm mentioned above (Skjern, Jutland, Denmark), where both the PTR-  
253 MS and the PAS were measuring continuously over 20 days. The dairy farm housed 360 cows  
254 with an average weight of 650 kg. The ventilation system consisted of natural and mechanical  
255 partial pit ventilation system (Rong et al., 2015).

256 For the field test, the PAS was combined with a Multiplexer 1309 (Lumasense Technology A/S,  
257 Denmark) to measure from several sampling points. The PAS and the PTR-MS were placed in  
258 a trailer next to the dairy farm. The PAS sample integration time was 5 s and the flushing time  
259 was 20 s. The air concentrations were measured by the PAS sequentially between two selected

260 locations inside the farm, one location in the pit ventilation, one location outside the farm. PTFE  
261 tubes of 20 meters and 8 mm OD were used for the sampling of air. The sampling lines were  
262 connected with the channels of the PAS multi-point sampler via continuously running PTFE  
263 membrane pumps to ensure constant flushing. VOCs (all VOCs showed in section 2.3 were  
264 included together with VOCs reported in previous studies (Malkina et al., 2011; Hafner et al.,  
265 2013)) and NH<sub>3</sub> were measured simultaneously by PTR-MS. Measurements were switched  
266 between the four measurement sampling lines (connecting to the four locations mentioned  
267 above) and the background (outside air beside the trailer) at 8 min intervals via a custom-built  
268 switching box. PTFE tubes were used for the PTR-MS sampling lines, which were connected  
269 to PTFE sampling lines before the PTFE membranes pumps. The switching box was equipped  
270 with a five-port channel selector (Bio-Chem Valve Inc, USA) controlled automatically by 24V  
271 outputs from the PTR-MS. A PTFE tube (ID 1 mm) was used to connect the switching box to  
272 the inlet sampling line (1-meter PEEK tube with ID 0.64 mm) of the PTR-MS. For selected  
273 compounds, calibration was performed for the PTR-MS before the field measurements using  
274 permeation tubes and reference gas mixtures. Permeation tubes (VICI Metronics, Inc., Houston,  
275 TX, USA) included acetic acid, propanoic acid, butanoic acid, pentanoic acid and 4-  
276 methylphenol. Gas mixtures (all 5 ppmv in nitrogen) included hydrogen sulfide (AGA,  
277 Copenhagen, Denmark), methanethiol (AGA, Copenhagen, Denmark), and dimethyl sulfide  
278 (Air Liquide, Horsens, Denmark). Details regarding the calibration procedures could be found  
279 in our previous study, with accuracies within 12% error and in most cases within 8% (Liu et al.,  
280 2018). VOC concentrations were determined directly by the PTR-MS, based on estimated  
281 reaction rate constants as described by Liu et al. (2018). Standard conditions as described

282 previously was applied and maintained for the PTR-MS (Feilberg et al., 2010). The mass  
 283 discrimination was calibrated and adjusted weekly by using a mixture of 14 aromatic  
 284 compounds between m/z (mass to charge ratio) 79 and 181 (P/N 34423-PI, Restek, Bellefonte,  
 285 PA). Selected ions were monitored with dwell time between 200 and 2000 ms during each  
 286 measurement cycle. Masses and dwell time selection was based on ion abundance in full scan  
 287 mode, relevant literature and experience regarding odorant compounds from dairy buildings as  
 288 well as from pig houses and pig slurry applications (Shaw et al., 2007; Chung et al., 2009; Liu  
 289 et al., 2014; Liu et al., 2018).



299 **Figure 2.** Ammonia test measurements by PAS, PTR-MS and CRDS. A: Background signals  
 300 measured in ammonia-free air. B: Intercomparison of ammonia concentrations measured by PTR-  
 301 MS and CRDS. C: Instrumental response of PTR-MS, PAS and CRDS instruments to a  
 302 rectangular ammonia concentration pulse.; D: Instrumental response of PAS instrument to a  
 303 stepwise increase in ammonia concentration (low concentration (3 tests; ~8.9 ppmv) and high  
 304 concentration (2 tests; 99.7 ppmv); Low Conc.-1, Low Conc.-2 and Low Conc.-3 point to the  
 305 vertical axis on the left, and to the upper horizontal axis; High Conc.-1 and High Conc.-2 point to  
 306 the vertical axis on the right, and to the lower horizontal axis; High Conc.-2 was tested without the  
 307 multiplexer). Data in B has been background-subtracted and the linear fits were least square fits  
 308 without error weighting.

### 309 3 Results and discussion

#### 310 3.1 Experiment 1: laboratory test on ammonia calibration

311 The instrumental baseline concentrations of ammonia-free zero air measured by PAS, CRDS  
312 and PTR-MS, respectively, are shown in Figure 2A, in which a very low background signal was  
313 observed for the CRDS instrument (around 1 ppbv) with a detection limit of 0.7 ppbv (3 times  
314 the standard deviation of the background). The higher background for ammonia measured from  
315 the PTR-MS is caused by the intrinsic formation of  $\text{NH}_4^+$  ( $m/z$  18) in the ion source (Norman  
316 et al., 2007). Nevertheless, the measured background signals for ammonia by the PTR-MS was  
317 very stable and could be subtracted to give a detection limit of 21 ppbv (3 times the standard  
318 deviation of the background). Among the three instruments, the PAS gave the highest  
319 background signal for ammonia (corresponding to  $502 \pm 140$  ppb), with a detection limit of 421  
320 ppbv (3 times the standard deviation of the background).

321 For the calibration test of ammonia, the ammonia concentrations simultaneously measured by  
322 the CRDS and the PTR-MS is shown in Figure 2B, in which the linearity ( $k = 0.96 \pm 0.005$ )  
323 and high correlation ( $R^2=0.999$ ) are generally very satisfactory for both instruments. The  
324 measured ammonia concentrations also agreed with expected ammonia concentrations from the  
325 ammonia reference gas within the uncertainty of 10% provided by the gas supplier.

326

327

328

329

330

331 **Table 1.** Instruments comparison regarding the specifications for ammonia measurements (SD =  
 332 standard deviation).

	LOD(3×SD; ppbv)	Upper limit (ppmv)	90% decay time (s)	Measurement time	1σ Accuracy*	Possible Interferences
Innova	421(200 <sup>*</sup> )	(-) <sup>A</sup>	1700-4000 (5.2-8.8 ppmv); 450-550 (100 ppmv)	Less than 2 min	16.4%	Non-targeted gases with IR spectra Overlapping
PTR-MS	21.5	10 <sup>#</sup>	70-80 (5.2 ppmv)	Less than 5 s	10.3%	intrinsic ion at m/z 18
Picarro	0.662	>20 <sup>&amp;</sup>	4.5-4.7 (5.2 ppmv)	Less than 2 s	10.2%	Negligible <sup>&amp;</sup>

333

334 \* - Accuracy propagated from uncertainty of the calibration standard gas of ammonia (10%),  
 335 uncertainty of mass flow controller (2%) used for gas dilution systems, and uncertainty of  
 336 instrumental quantities of ammonia (12.8%, 1.6% and 0.2% for Innova, PTR-MS and Picarro,  
 337 respectively). It should be noted that the uncertainty associated with the comparison to the  
 338 standard gas did not take into account the interferences by other livestock gases on the Innova.

339 A - Not specified by the producer.

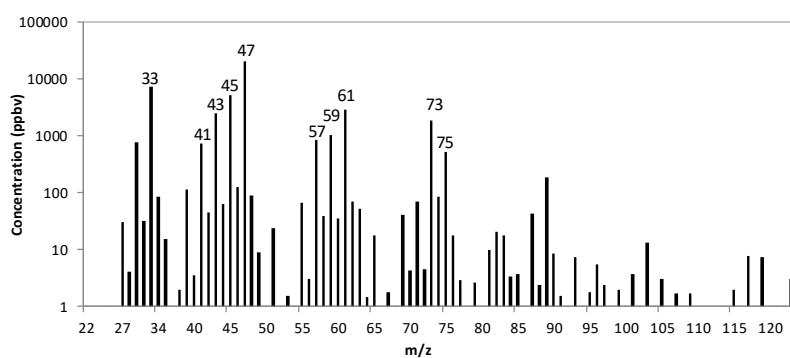
340 # - According to the concentration calculation assumption and producer suggestion, total gas  
 341 concentration should be lower than 10 ppmv, otherwise dilution is needed.

342 &- According to Kamp et al., 2019.

343 For the signal decay test, the instrument decay times for ammonia measurements by PAS,  
 344 CRDS and PTR-MS were measured simultaneously under a static ammonia concentration of  
 345 5.2 ppmv. As shown in Figure 2C, ammonia measured by the CRDS showed the shortest decay  
 346 time while the PAS gave by far the longest decay time. The estimated decay time is shown in  
 347 Table 1, in which the 90% decay time (time for the concentration to decrease by 90%) for  
 348 ammonia measured by the CRDS is around 4.5 - 4.7 second, with the 90% decay time from the  
 349 PTR-MS estimated to be 70 to 80 seconds. The decay time for ammonia measured by the PAS  
 350 was remarkably longer, with an estimated 90% decay time of around 30 minutes to more than  
 351 an hour (for four individual tests with ammonia concentration ranged from 5.2 to 8.8 ppmv).  
 352 When much higher ammonia concentration was used (99.7 ppmv), the 90% decay time  
 353 measured by the PAS was shorter (450 to 550 seconds). This result is consistent with the  
 354 response time tests under two levels of input ammonia concentrations (~ 8.9 ppmv and 99.7



355 ppmv, respectively), with the response time much shorter when the ammonia concentration is  
356 higher, as shown in Figure 2D. Besides, the multiplexer attached to the PAS seemed to increase  
357 the response time, as also shown in Figure 2D. However, a very high concentration of about  
358 100 ppmv is not expected in agricultural applications.



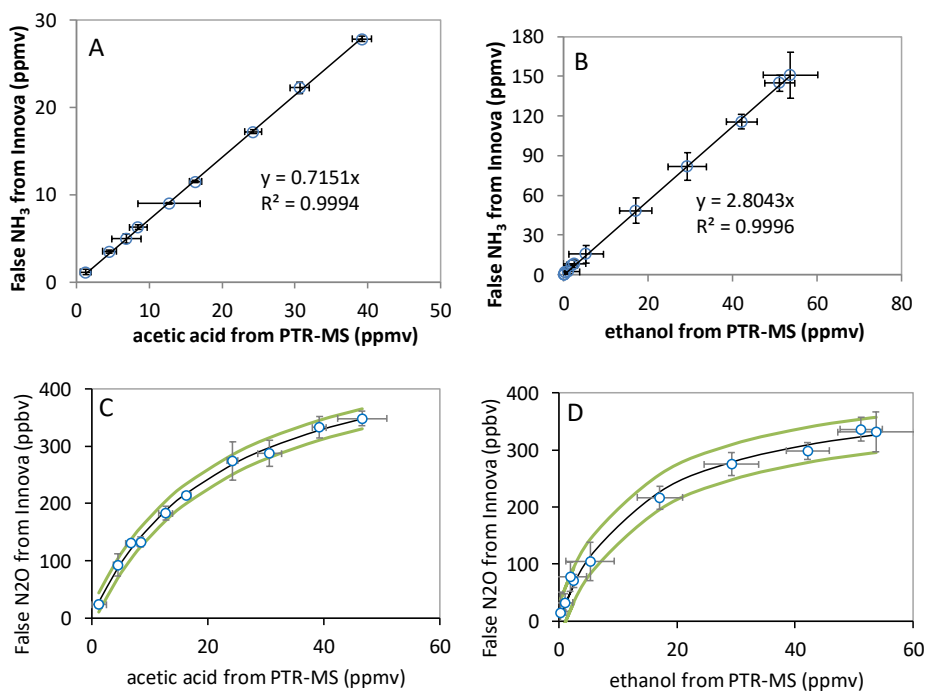
359  
360 **Figure 3.** A scan example of the feeding material of silage by using headspace technique measured by  
361 the PTR-MS. The m/z 47 is corrected for ethanol fragmentations formed in the PTR-MS through  
362 calibration. Selected VOCs for the test in this study were ethanol, methanol, acetaldehyde, acetic acid,  
363 2-butanone, acetone, propanol and butanol.

364

### 365 **3.2 Experiment 2: VOCs selection test**

366 The tested VOCs were selected according to a scan test of the headspace from the feeding  
367 material of maize silage performed by the PTR-MS, as shown in Figure 3. Due to the  
368 fragmentation of ethanol in the PTR-MS measurement (around 10%) (Inomata and Tanimoto,  
369 2009), the concentration corresponding to mass 47 was corrected based on direct calibration  
370 under the assumption that mass 47 is solely due to ethanol. The highest peaks of the scan were  
371 at masses (m/z): 47, 33, 45, 61, 43, 73, 59, 75, 57 and 41. From the VOCs typically found in  
372 the highest concentrations in barns and feeding material (Shaw et al., 2007; Chung et al.,  
373 2009; Howard et al., 2010; Malkina et al., 2011; Hafner et al., 2013) and the scan results, a list  
374 of VOCs were selected. The following VOCs were selected for the interference tests of non-  
375 targeted VOC on ammonia measurement by the PAS: ethanol, methanol, acetaldehyde, acetic

376 acid, 2-butanone, acetone, 1-propanol and 1-butanol. Compounds such as ethanol, methanol,  
 377 acetic acid and 1-propanol are typically measured in cattle barns and feeding materials in high  
 378 concentrations (Shaw et al., 2007; Ngwabie et al., 2008; Howard et al., 2010; Hafner et al.,  
 379 2013).



398 **Figure 4.** Examples for the interference calibration from non-targeted VOC on NH<sub>3</sub> (A & B) and  
 399 N<sub>2</sub>O (C & D) measured by the PAS. The VOC concentration on the horizontal axis was measured  
 400 by the PTR-MS, while the NH<sub>3</sub> and N<sub>2</sub>O concentrations on vertical axis were from false signals  
 401 measured meanwhile by the PAS. A: The interference calibration for acetic acid on NH<sub>3</sub>; B: The  
 402 interference calibration for ethanol (corrected for fragments through calibration) on NH<sub>3</sub>; C: The  
 403 interference calibration for ethanol (corrected for fragments through calibration) on N<sub>2</sub>O; D: The  
 404 interference calibration for acetic acid on N<sub>2</sub>O. In C & D, the red line indicated the fit curve by  
 405 equation  $y=kx/(x+m)$ , and the green and purple curves indicated 95% confidence range. The plotted  
 406 error bars represent the standard deviations for the measured VOC by the PTR-MS under a  
 407 selected VOC level (x-axis) and for the measured NH<sub>3</sub>/N<sub>2</sub>O level by the PAS meanwhile (y-  
 408 axis). Data were all background-subtracted and the linear fits were least square fits without error  
 409 weighting.

410

### 411 3.3 Experiment 3: Laboratory test for empirical relationships

412 The interference of non-targeted VOC on ammonia measurement by the PAS was investigated

413 using single VOC-containing air as inlet measured simultaneously by PAS, PTR-MS and CRDS,  
 414 as shown in the setup in Figure 1. An example of the interference test can be seen in Figure S1,  
 415 where acetic acid was measured simultaneously by the three instruments under various  
 416 concentration levels. Concentration dependent interference was clear for acetic acid on PAS  
 417 ammonia measurements.

418 **Table 2.** Obtained empirical relationships (slope) describing the functional dependence of the  
 419 interference in the measurement of the target compound (e.g., NH<sub>3</sub>) by PAS on non-targeted VOC  
 420 concentrations. The value in the brackets indicated the uncertainty (SD of the slope) of the linear fit,  
 421 except for N<sub>2</sub>O where correlation coefficient is shown. N is the number of VOC concentration levels  
 422 tested for determination of empirical relationships. Nonlinear fit was given for N<sub>2</sub>O, where 'x' is  
 423 measured VOC concentration and 'y' is the false concentration measured by PAS. The concentration  
 424 range covered for the tested VOC is as follows: ethanol (7 ppbv-58 ppmv); methanol (5 ppbv-45  
 425 ppmv); acetic acid (3 ppbv - 48 ppmv); acetaldehyde (8 ppbv-38 ppmv); 2-butanone (3 ppbv - 60  
 426 ppmv); acetone (4 ppbv - 48 ppmv); 1-propanol (5 ppbv - 55 ppmv); 1-butanol (6 ppbv - 52 ppmv).

Compound	N	NH <sub>3</sub>	CH <sub>4</sub>	N <sub>2</sub> O (y: ppbv; x: ppmv)	CO <sub>2</sub>	SF <sub>6</sub>
ethanol	10	2.81(0.02)	1.88(0.01)	$y=411x/(x+14)$ (0.93)	0.40(0.02)	-0.014(0.002)
methanol	9	3.29(0.72)	3.81(0.67)	$y=99x/(x+9)$ (0.78)	0.45(0.17)	-0.15(0.02)
acetic acid	10	0.72x(0.01)	-3.14x(0.08)	$y=514x/(x+22)$ (0.95)	0.39(0.03)	0.31(0.01)
acetaldehyde	4	(-)	-0.85(0.45)	$y=317x/(x+31)$ (0.98)	(-)	0.044(0.021)
2-butanone	4	-0.13x(0.003)	-4.02(0.04)	$y=311x/(x+26)$ (1.00)	-0.61(0.18)	0.23(0.005)
acetone	6	0.02(0.001)	2.10(0.13)	$y=104x/(x+4)$ (0.99)	(-)	0.015(0.001)
1-propanol	5	2.41(0.21)	2.95(0.38)	$y=3569x/(x+602)$ (1.00)	0.25(0.21)	-0.064(0.012)
1-butanol	7	2.66(0.05)	3.07(0.09)	$y=807x/(x+73)$ (0.99)	(-)	-0.061(0.004)
methanol(N <sub>2</sub> )	4	1.03(0.31)	1.46(0.22)	(-)	0.35(0.24)	-0.056(0.010)

427  
 428 In principle, establishing empirical correction factors for each specific compound could be used  
 429 to minimize the interferences of VOCs on the target gas measurements on a specific instrument  
 430 with the same filter specifications. This requires, however, that VOC concentrations be  
 431 measured simultaneously by expensive analyzers such as PTR-MS and will in any case result  
 432 in higher uncertainties due to accumulated uncertainties from multiple interference  
 433 relationships. Figure 4A & B show two examples of the calibration lines for acetic acid and

434 ethanol, from which an empirical relationship (ER) between the false ammonia concentration  
435 and the tested compound could be obtained (ER=0.72 for acetic acid and ER=2.8 for ethanol).

436 A linear response of the ammonia interference was observed for all the tested compounds and  
437 they had generally low SD for the slope the linear fits. The ER for ammonia interference by  
438 other tested VOCs can be found in Table 2, where ethanol, methanol, 1-propanol and 1-butanol  
439 give the highest false signals on ammonia measured by the PAS, with ER of 2.8, 3.3, 2.4 and  
440 2.7, respectively. Due to the fact that these compounds are often found in cattle barns and feed  
441 silage even in the level of ppmv, especially for ethanol, methanol and 1-propanol (Rabaud et  
442 al., 2003; Ngwabie et al., 2008; Howard et al., 2010; Hafner et al., 2013), severe interference  
443 on ammonia measured by PAS therefore will occur. While acetic acid gave significant false  
444 signals on ammonia (ER=0.72), acetone only showed little interference on ammonia (ER=0.02).

445 Meanwhile, negative false signals were observed for ammonia by 2-butanone (ER=-0.13). Such  
446 negative interferences can usually be explained by the internal cross compensation procedure  
447 for one target filter (first target filter, such as NH<sub>3</sub> filter) on positive artifacts at another target  
448 filter (second target filter, such as CH<sub>4</sub> filter) caused by non-target gas (such as VOC) on the  
449 second target filter. This physical explanation was included in a few relevant references such  
450 as Zhao et al. (2012). Interestingly, the empirical relationship for false ammonia by methanol  
451 in nitrogen matrix is significantly different from that by methanol presented in air matrix  
452 (ER=1.03 vs 3.29). This observation is possibly related to the relatively rapid vibrational energy  
453 transfer between the VOC and oxygen (Harren et al., 2000). While nitrogen has a vibrational  
454 frequency around 2360 cm<sup>-1</sup>, oxygen has a vibrational frequency of 1554 cm<sup>-1</sup> with only 170  
455 collisions needed to transfer energy to the vibrational mode of O<sub>2</sub> (Lambert, 1977).

456 Besides the interferences on ammonia by the non-targeted VOCs, other target gases also  
457 showed various levels of interferences, as also indicated by previous studies (e.g., Zhao et al.,  
458 2012; Hassouna et al., 2013). Because target gases may have more overlap for the infrared  
459 spectrum, the primary interference on one target gas caused by the overlap with non-targeted  
460 VOCs could therefore influence and cause secondary interference on other target gases (Zhao  
461 et al., 2012; Adamsen, 2018). Still, in theory, empirical relationships could be obtained for the  
462 interfered gases by the tested VOCs. Specifically, for the interference on methane by non-  
463 targeted methanol, 1-butanol, 1-propanol, acetone and ethanol showed positive false signals  
464 (ER=3.8, 3.1, 3.0, 2.1, 1.9, respectively). 2-butanone, acetic acid and acetaldehyde showed  
465 negative false signals to methane, with ER equal to -4.02, -3.14 and -0.85, respectively. An  
466 explanation for the negative false signals could be that absorption takes place in the band for  
467 H<sub>2</sub>O correction (Adamsen, 2018). All interferences on methane are shown in Table 2. For  
468 methanol in nitrogen, the calibration showed a significant difference compared to air (ER=1.46  
469 vs. 3.81).

470 Meanwhile, the non-targeted VOC also caused false signals on nitrous oxide signals, with a  
471 much lower level of interference. Furthermore, the calibrations of the nitrous oxide interference  
472 by the non-targeted VOCs seemed not to be following linear relationships. For examples, Figure  
473 4C & D showed the false signals of nitrous oxide caused by ethanol and acetic acid. A non-  
474 linear relationship exists between nitrous oxide interference and VOC concentration. The  
475 curves could be well fitted to the non-linear equation of  $y = \frac{kx}{x+m}$ , where k represents the  
476 maximum interference on nitrous oxide by the single VOC, m represents the half-saturation  
477 constant indicating the level higher at which the VOC concentration could cause half of the

478 maximum interference on nitrous oxide. As shown in Table 2, all tested VOCs showed positive  
479 non-linear interference to the nitrous oxide signals, and 1-butanol showed the highest maximum  
480 interference on nitrous oxide. Interestingly, no interference was observed for nitrous oxide  
481 when methanol was presented in a nitrogen matrix, while a relatively lower level of interference  
482 by methanol was observed for nitrous oxide when presented in atmospheric air.

483 Furthermore, some of the tested VOCs also caused interference on carbon dioxide measured by  
484 the PAS. The background of carbon dioxide was considered as unchanged during the  
485 interference tests. While methanol, ethanol, acetic acid and 1-propanol caused positive false  
486 signals for carbon dioxide measured by the PAS (ER = 0.45, 0.40, 0.39, 0.25, respectively), 2-  
487 butanone caused negative false signals with ER = -0.61 (Table 2). Other tested VOCs, including  
488 acetone, acetaldehyde and 1-butanol, did not show interferences on carbon dioxide measured  
489 by the PAS. This is likely because no overlap of the gas infrared adsorption spectra exists  
490 between these VOCs and carbon dioxide. As expected, methanol in nitrogen also caused  
491 interference on carbon dioxide (ER = 0.35) slightly lower than methanol in air.

492 Besides, SF<sub>6</sub> measurements were interfered by the tested non-targeted VOC, with lower  
493 empirical relationship obtained compared to NH<sub>3</sub>, CH<sub>4</sub>, N<sub>2</sub>O and CO<sub>2</sub>. Acetic acid and 2-  
494 butanone caused the highest interferences on SF<sub>6</sub>, with ER of 0.31 and 0.23, respectively. Other  
495 tested VOCs caused significantly less interference on SF<sub>6</sub>, among which methanol gave the  
496 highest negative ER of -0.15. Again, the methanol in nitrogen gave a significantly lower level  
497 of interference on SF<sub>6</sub> compared to methanol in air (ER = -0.056 vs -0.15).

498 Overall, the tested non-target VOCs in this study caused significant interference on target gases,  
499 of which ammonia and methane were influenced to the largest degree. Even though less

500 interference was observed for nitrous oxide, this could still cause problems due to the typically  
501 low concentration level of this compound in e.g. livestock facilities or soil (Iqbal et al., 2013;  
502 Rong et al., 2014).

503

504

505

506

507

508

509

510

511

512

513

514

515

516

517

518

519

520

521

522

523

524

525

526

527

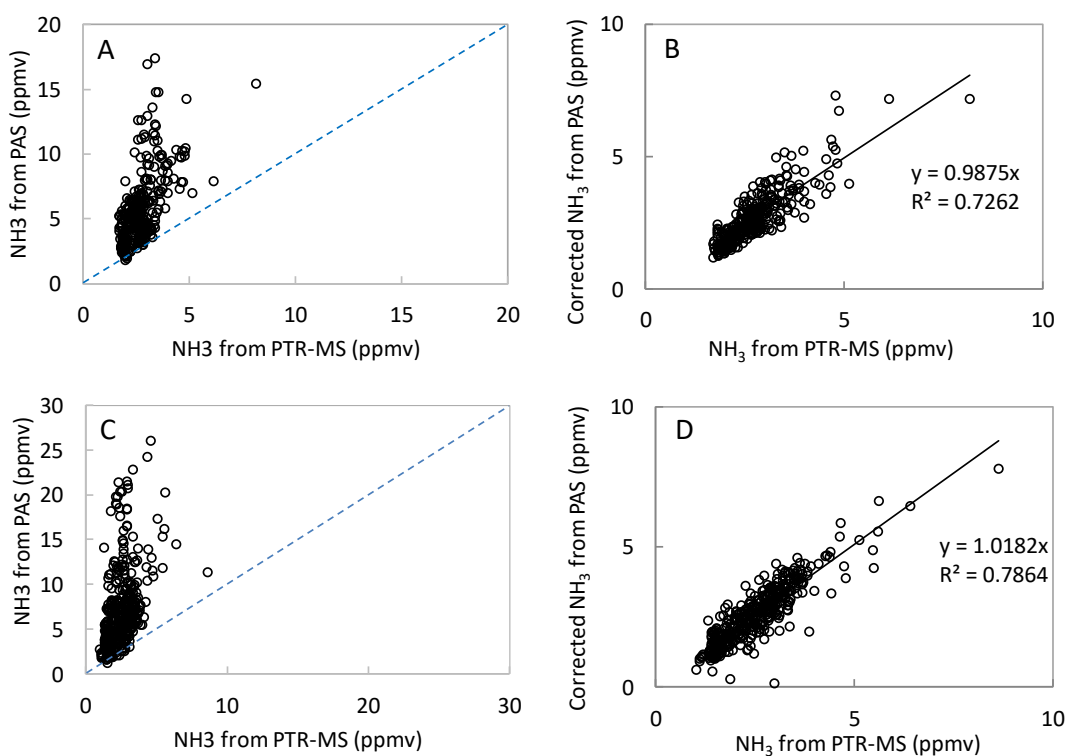
528

529 **Figure 5.** NH<sub>3</sub> concentrations measured by the PAS (vertical axis) and by the PTR-MS (horizontal  
530 axis) in the field measurement from Location One before the correction by the tested non-targeted  
531 VOCs (A) and after the correction by the tested non-targeted VOCs (B), and from Location Two  
532 before the correction by the tested non-targeted VOCs (C) and after the correction by the tested non-  
533 targeted VOCs (D). Data from B and D were background corrected and the linear fits were least  
534 square fits without error weighting.

535

### 536 3.4 Experiment 4: Field test for validation of empirical relationships

537 During the field test in the dairy barn, the ammonia measurements by PAS and PTR-MS were



538 compared to each other for one location in the pit and two locations (Location One and Location  
539 Two) in the barn. Figure S2 shows ammonia concentration measured by PAS and PTR-MS at  
540 the pit ventilation. In the pit ventilation, low concentrations of VOCs were generally obtained  
541 and relatively high concentrations of ammonia were observed for both instruments. Thus, no  
542 significant interferences were observed for ammonia measured by the PAS, and ammonia  
543 measurements by PAS and PTR-MS showed a good agreement as shown in Figure S2. However,  
544 for the two measurement points inside the barn, significantly higher ammonia concentrations  
545 were obtained from PAS compared to the concentrations measured by PTR-MS (Figure 5 A &  
546 C). Table S2 showed the percentage for each range of ratio of PAS/PTR-MS concentrations for  
547 the data shown in Figure 5 A & C, where ratio of PAS/PTR-MS concentrations mostly within  
548 1-4. The higher ammonia concentration observed for the PAS measurement is ascribed to  
549 interferences from VOCs, some of which had high concentrations, especially for ethanol as  
550 shown in Table 3. The relation between the ammonia concentrations measured by PAS and the  
551 ethanol concentrations measured by PTR-MS were highly correlated for both measurement  
552 locations, with slopes close to 3 (3.0 and 3.1; see Figure S3). These two numbers are generally  
553 close to the empirical relationship obtained for ethanol ( $ER = 2.8$ ). The empirical relationships  
554 obtained in 'Experiment 3' were used for data correction of ammonia measurement by PAS  
555 since the instrument configurations were kept the same. Thus, the interference of the VOCs on  
556 ammonia measurement by PAS could be estimated from the empirical relationships obtained in  
557 'Experiment 3' and used to correct the ammonia data. Figure 5B & D show the corrected  
558 ammonia concentrations measured by PAS by using the empirical relationships, together with  
559 the measured ammonia concentration by the PTR-MS for both measurement locations. The



560 corrected ammonia concentrations from the PAS are generally in good agreement with the  
561 ammonia concentration measured by the PTR-MS, with slopes close to 1 (0.99 and 1.02). It  
562 should be noted that although the empirical relationships were obtained for single VOC  
563 interferences on ammonia measurement by PAS, they were treated as being additive under field  
564 conditions where multiple VOCs presented. Ethanol dominated the VOC composition in  
565 general, but other types of VOC also contribute significantly. The average ratio of ethanol  
566 concentration to the sum of the 8 VOCs (tested in the lab with obtained empirical relationships)  
567 was 0.64 ( $\pm 0.11$ ) for Location Two in the field study. This single application suggests that the  
568 interference is close to additive, but further investigation is needed to confirm this finding. The  
569 cattle barn experiment validated that correction from major VOCs is necessary for reliable PAS  
570 measurements. In principle, it is possible to estimate the interference on NH<sub>3</sub> measured by PAS  
571 measurements in field applications. However, it should be noted that a lot of redundant work is  
572 needed to make this correction if only NH<sub>3</sub> concentration is measured since the concentrations  
573 of several VOCs need to be known to achieve a proper correction.

574

575 **Table 3.** Average concentrations ( $\pm$  standard deviation) of selected VOCs during the field test in the  
576 dairy cattle barn for the two sampling locations 1 & 2, both of which are located inside the barn. The  
577 standard deviation applies to the mean values.

Compound	Concentrations (ppbv)	
	Location 1	Location 2
ethanol	1421±946	1622±1355
methanol	237.2±150.2	241.1±192.3
acetic acid	57.2±41.3	69.4±61.6
acetaldehyde	98.8±81.2	92.2±83.7
2-butanone	19.1±11.0	17.2±13.1
acetone	77.9±30.2	52.1±24.9
1-propanol	71.0±45.2	71.8±67.7
1-butanol	22.2±10.1	16.3±11.8
hydrogen sulfide	12.1±9.7	11.3±8.4
trimethylamine	8.6±3.5	5.7±3.1
dimethyl sulfide	15.1±9.2	14.3±9.8
4-methylphenol	5.2±2.1	3.8±2.2

578

579

#### 580 **4 Conclusions**

581 When measuring NH<sub>3</sub> and greenhouse gas emissions (CH<sub>4</sub>, N<sub>2</sub>O and CO<sub>2</sub>) by PAS, non-target

582 VOCs may interfere significantly with the target gases causing inaccurate results. To confirm

583 and determine the magnitude of interferences, experiments have been conducted by

584 simultaneously using a PAS and a PTR-MS. Results from these experiments provide useful

585 guidelines concerning interferences caused by non-targeted VOCs. The results demonstrate that

586 ethanol, methanol, 1-butanol, 1-propanol and acetic acid are causing the most significant

587 interferences on NH<sub>3</sub> measured by PAS. A field test in a cattle barn validated the interference

588 caused by VOCs on NH<sub>3</sub> measurement by PAS by simultaneously measuring VOCs with PTR-

589 MS.

590

591 *Code and data availability.* Data and code are available upon request to the corresponding

592 author.

593 *Supplement.* The supplementary information is available free of charge at DOI: .

594

595 *Author contributions.* DL, LR and AF designed the setup for the experiments performed; LR,  
596 JK and AC contributed to setting up and conducting experiments and acquiring data; DL, AF,  
597 JK, XK and APA contributed to writing the manuscript, data interpretation and data analysis;  
598 LR, AF and JK assisted in data analysis and manuscript editing.

599

600 *Competing interests.* The authors declare that they have no conflicts of interest.

601

602 *Acknowledgements.* Part of this work was supported by National Natural Science Fund of  
603 China (No. 31672468) and Thousand Talents Program (Youth Project 2016).

604

## 605 **References**

606 Adamsen, A.P. Measurement of climate gases from livestock barns with infrared photo-acoustic  
607 spectrometry (In Danish: Måling af klimagasser fra stalde med infrarød fotoakustisk  
608 spektrometri), Technical Report, SEGES, December, 2018.

609 Aneja, V. P., Schlesinger, W. H., and Erisman, J. W.: Effects of agriculture upon the air quality  
610 and climate: research, policy, and regulations, *Environ. Sci. Technol.*, 43, 4234–4240,  
611 <https://doi.org/10.1021/es8024403>, 2009.

612 Angela, E., Di, F. C., Mario, L. P., and Gaetano, S.: Photoacoustic Spectroscopy with Quantum  
613 Cascade Lasers for Trace Gas Detection, *Sensors-Basel*, 6, 1411–1419,  
614 <https://doi.org/10.3390/s6101411>, 2006.

615 Inomata S., Tanimoto H.: A deuterium-labeling study on the reproduction of hydronium ions in

616 the PTR-MS detection of ethanol, *Int. J. Mass Spectrom.*, 285, 95-99, [http://doi.org/](http://doi.org/10.1016/j.ijms.2009.05.001)  
617 [10.1016/j.ijms.2009.05.001](http://doi.org/10.1016/j.ijms.2009.05.001), 2009.

618 Berden, G., Peeters, R., and Meijer, G.: Cavity ring-down spectroscopy: Experimental schemes  
619 and applications, *Int. Rev. Phys. Chem.*, 19, 565–607,  
620 <https://doi.org/10.1080/014423500750040627>, 2000.

621 Blake, R. S., Monks, P. S., and Ellis, A. M.: Proton-transfer reaction mass spectrometry, *Chem.*  
622 *Rev.*, 109, 861–896, <https://doi.org/10.1002/chin.200923275>, 2009.

623 Blanes-Vidal, V., Topper, P. A., and Wheeler, E. F.: Validation of ammonia emissions from dairy  
624 cow manure estimated with a non-steady-state, recirculation flux chamber with whole-  
625 building emissions, *T. ASABE*, 50, 633–640, <https://doi.org/10.13031/2013.22652>, 2007.

626 Bouwman, A. F., Lee, D. S., Asman, W. A. H., Dentener, F. J., Van, D. H. K. W., and Olivier, J.  
627 G. J.: A global high-resolution emission inventory for ammonia, *Global Biogeochem. Cy.*,  
628 11, 561–587, <https://doi.org/10.1029/97GB02266>, 1997.

629 California Air Resources Board (CARB):. Manufacturer Notification. Mail-Out #MSO 2000-  
630 08, CARB: Sacramento, CA, USA, Available online:  
631 <http://www.arb.ca.gov/msprog/mailouts/mso0008/mso0008.pdf>, 2000.

632 Chadwick, D., Sommer, S., Thorman, R., Fanguero, D., Cardenas, L., Amon, B., and  
633 Misselbrook, T.: Manure management: Implications for greenhouse gas emissions, *Anim.*  
634 *Feed Sci. Tech.*, 166-167, 514–531, <https://doi.org/10.1016/j.anifeedsci.2011.04.036>, 2011.

635 Christensen J. The Brüel&Kjær Photoacoustic Transducer System and its Physical Properties.  
636 Brüel&Kjær Technical Review, 1, 1990a.

637 Christensen J. Optical filters and their use with the type 1302 type 1306 photoacoustic gas

638 monitors. Brüel&Kjær Technical Review, 2, 1990b.

639 Chung, M.Y., Beene, M., Ashkan, S., Krauter, C., and Hasson, A.S.: Evaluation of non-enteric  
640 sources of non-methane volatile organic compound (NMVOC) emissions from dairies,  
641 Atmos. Environ., 44, 786–794, <https://doi.org/10.1016/j.atmosenv.2009.11.033>, 2009.

642 Cortus E.L., Jacobson L.D., Hetchler B.P., and Heber A.J.: Emission monitoring methodology  
643 at a NAEMS dairy site, with an assessment of the uncertainty of measured ventilation rates,  
644 ASABE - 9th International Livestock Environment Symposium, 583-590,  
645 <https://doi.org/10.13031/2013.41578>, 2012.

646 De Gouw J., and Warneke C.: Measurements of volatile organic compounds in the earth's  
647 atmosphere using proton-transfer-reaction mass spectrometry, Mass Spectrom. Rev., 26,  
648 223–257, <https://doi.org/10.1002/mas.20119>, 2007.

649 EMEP, Agency: EMEP/EEA air pollutant emission inventory guidebook - 2013. *Luxembourg:*  
650 *Publications Office of the European Union*, 3B: Manure management,  
651 [https://www.eea.europa.eu/publications/emep-eea-guidebook-2013/part-b-sectoral-](https://www.eea.europa.eu/publications/emep-eea-guidebook-2013/part-b-sectoral-guidance-chapters/4-agriculture/3-b-manure-management/view)  
652 [guidance-chapters/4-agriculture/3-b-manure-management/view](https://www.eea.europa.eu/publications/emep-eea-guidebook-2013/part-b-sectoral-guidance-chapters/4-agriculture/3-b-manure-management/view), 2013.

653 Emmenegger, L., Mohn J., Sigrist M., Marinov D., Steinemann U., Zumsteg F., and Meier M.:  
654 Measurement of ammonia emissions using various techniques in a comparative tunnel study,  
655 Int. J. Environ. Pollut., 22, 326–341, <https://doi.org/10.1504/IJEP.2004.005547>, 2004.

656 Erisman, J. W., Bleeker, A., Galloway, J., and Sutton, M. S.: Reduced nitrogen in ecology and  
657 the environment, Environ. Pollut., 150, 140–149,  
658 <https://doi.org/10.1016/j.envpol.2007.06.033>, 2007.

659 Feilberg A., Liu D., Adamsen A.P.S., Hansen M.J., and Jonassen K.E.N.: Odorant emissions

660 from intensive pig production measured by online proton-transfer-reaction mass  
661 spectrometry, *Environ. Sci. Technol.*, 44, 5894–5900, <https://doi.org/10.1021/es100483s>,  
662 2010.

663 Fle'chard, C. R., Neftel, A., Jocher, M., Ammann, C., and Fuhrer, J.: Bi-directional  
664 soil/atmosphere N<sub>2</sub>O exchange over two mown grassland systems with contrasting  
665 management practices, *Global Change Biol.*, 11, 2114–2127, [https://doi.org/10.1111/j.1365-](https://doi.org/10.1111/j.1365-2486.2005.01056.x)  
666 2486.2005.01056.x, 2010.

667 Hafner S.D., Howard C., Muck R.E., Franco R.B., Montes F., Green P.G., Mitloehner F., Trabue,  
668 S.L., and Rotz C.A.: Emission of volatile organic compounds from silage: Compounds,  
669 sources, and implications, *Atmos. Environ.*, 77, 827–839,  
670 <https://doi.org/10.1016/j.atmosenv.2013.04.076>, 2013.

671 Hafner, S. D., Montes, F., Rotz, C. A., and Mitloehner, F.: Ethanol emission from loose corn  
672 silage and exposed silage particles. *Atmos. Environ.*, 44, 4172–4180,  
673 <https://doi.org/10.1016/j.atmosenv.2010.07.029>, 2010.

674 Harren F.J.M., Cotti G., Oomens J., and Hekkert S.L.: Photoacoustic Spectroscopy in Trace Gas  
675 Monitoring, in *Encyclopedia of Analytical Chemistry*, R.A. Meyers (Ed.), 2203–2226,  
676 ©JohnWiley & Sons Ltd, Chichester, 2000.

677 Hassouna, M., Espagnol, S., Robin, P., Paillat, J. M., Levasseur, P., and Li, Y.: Monitoring NH<sub>3</sub>,  
678 N<sub>2</sub>O, CO<sub>2</sub> and CH<sub>4</sub> emissions during pig solid manure storage and effect of turning,  
679 *Compost Sci. Util.*, 16, 267–274, <https://doi.org/10.1080/1065657X.2008.10702388>, 2008.

680 Hassouna, M., Robin, P., Charpiot, A., Edouard, N., and Méda, B.: Infrared photoacoustic  
681 spectroscopy in animal houses: Effect of non-compensated interferences on ammonia,

682 nitrous oxide and methane air concentrations, *Biosyst. Eng.*, 114, 318–326,  
683 <https://doi.org/10.1016/j.biosystemseng.2012.12.011>, 2013.

684 Heber A.J., Ni J.-Q., Lim T.T., Tao P.-C., Schmidt A.M., Koziel J.A., Beasley D.B., Hoff, S.J.,  
685 Nicolai, R.E., Jacobson, L.D., and Zhang Y.: Quality assured measurements of animal  
686 building emissions: Gas concentrations, *J. Air Waste Manage.*, 56, 1472–1483,  
687 <https://doi.org/10.1080/10473289.2006.10465680>, 2006.

688 Heyden, C. V. D., Brusselman, E., Volcke, E. I. P., and Demeyer, P.: Continuous measurements  
689 of ammonia, nitrous oxide and methane from air scrubbers at pig housing facilities, *J.*  
690 *Environ. Manage.*, 181, 163–171, <https://doi.org/10.1016/j.jenvman.2016.06.006>, 2016.

691 Howard, C. J., Kumar, A., Malkina, I., Mitloehner, F., Green, P. G., Flocchini, R. G., and  
692 Kleman, M. J.: Reactive organic gas emissions from livestock feed contribute significantly  
693 to ozone production in central California, *Environ. Sci. Technol.*, 44, 2309–2314,  
694 <https://doi.org/10.1021/es902864u>, 2010.

695 Hutchings, N. J., Sommer, S. G., Andersen, J. M., and Asman, W. A. H.: A detailed ammonia  
696 emission inventory for Denmark, *Atmos. Environ.*, 35, 1959–1968,  
697 [https://doi.org/10.1016/S1352-2310\(00\)00542-2](https://doi.org/10.1016/S1352-2310(00)00542-2), 2001.

698 Insam, H., and Seewald, M. S. A.: Volatile organic compounds (VOCs) in soils, *Biol. Fert. Soils*,  
699 46, 199–213, <https://doi.org/10.1007/s00374-010-0442-3>, 2010.

700 Iqbal, J., Castellano, M.J., and Parkin, T.B.: Evaluation of photoacoustic infrared spectroscopy  
701 for simultaneous measurement of N<sub>2</sub>O and CO<sub>2</sub> gas concentrations and fluxes at the soil  
702 surface, *Global Change Biol.*, 19, 327–336, <https://doi.org/10.1111/gcb.12021>, 2013.

703 Jie, D. F., Wei, X., Zhou, H. L., Pan, J. M., and Ying, Y. B.: Research progress on interference

704 in the detection of pollutant gases and improving technology in livestock farms: A review,  
705 *Appl. Spectrosc. Rev.*, 52,101–122, <https://doi.org/10.1080/05704928.2016.1208213>, 2016.

706 Joo H.S., Ndegwa P.M., Neerackal G.M., Wang X., and Harrison J.H.: Effects of manure  
707 managements on ammonia, hydrogen sulfide and greenhouse gases emissions from the  
708 naturally ventilated dairy barn, *ASABE*, 2, 1302-1311,  
709 <https://doi.org/10.13031/aim.20131593447>, 2013.

710 Kamp, J.N., Chowdhury, A., Adamsen, A.P.S., Feilberg, A.: Negligible influence of livestock  
711 contaminants and sampling system on ammonia measurements with cavity ring-down  
712 spectroscopy. *Atmos. Meas. Tech.*, 12, 2837–2850, [https://doi.org/10.5194/amt-12-2837-](https://doi.org/10.5194/amt-12-2837-2019)  
713 2019, 2019.

714 Lambert J.D.: *Vibrational and Rotational Relaxation in Gases*, Clarendon Press, Oxford, **1977**.

715 Lin, X., Zhang, R., Jiang, S., El-Mashad, H., and Xin, H.: Emissions of ammonia, carbon  
716 dioxide and particulate matter from cage-free layer houses in California, *Atmos. Environ.*,  
717 152, 246–255, <https://doi.org/10.1016/j.atmosenv.2016.12.018>, 2017.

718 Liu D., Lokke M.M., Leegaard Riis A., Mortensen K., and Feilberg A.: Evaluation of clay  
719 aggregate biotrickling filters for treatment of gaseous emissions from intensive pig  
720 production, *J. Environ. Manage.*, 136, 1–8, <https://doi.org/10.1016/j.jenvman.2014.01.023>,  
721 2014.

722 Liu, D., Nyord, T., Rong, L., and Feilberg, A.: Real-time quantification of emissions of volatile  
723 organic compounds from land spreading of pig slurry measured by PTR-MS and wind  
724 tunnels, *Sci. Total. Environ.*, 639, 1079–1087,  
725 <https://doi.org/10.1016/j.scitotenv.2018.05.149>, 2018.



726 Lumasense.: Photoacoustic Gas Monitor - INNOVA 1412i.  
727 [http://www.lumasenseinc.com/FR/produits/gas-sensing/gas-monitoring-](http://www.lumasenseinc.com/FR/produits/gas-sensing/gas-monitoring-instruments/photoacoustic-spectroscopy-pas/photoacoustic-gas-monitor-innova-1412i/)  
728 [instruments/photoacoustic-spectroscopy-pas/photoacoustic-gas-monitor-innova-1412i/](http://www.lumasenseinc.com/FR/produits/gas-sensing/gas-monitoring-instruments/photoacoustic-spectroscopy-pas/photoacoustic-gas-monitor-innova-1412i/).  
729 Accessed 18<sup>th</sup> November, 2018.

730 Malkina, I.L., Kumar, A., Green, P.G., and Mitloehner, F.M.: Identification and quantitation of  
731 volatile organic compounds emitted from dairy silages and other feedstuffs, *J. Environ. Qual.*,  
732 40, 28, <https://doi.org/10.2134/jeq2010.0302>, 2011.

733 Mathot, M., Decruyenaere, V., Lambert, R., Stilmant, D. Emissions de CH<sub>4</sub>, N<sub>2</sub>O et NH<sub>3</sub> en  
734 e´tables et lors du stockage des engrais de ferme de ge´nisses Blanc Bleu Belge. Paper  
735 presented at the 14e`me Journe´es 3R, Paris, 2007.

736 Melse, R. W., and Werf, A. W. V. D.: Biofiltration for mitigation of methane emission from  
737 animal husbandry, *Environ. Sci. Technol.*, 39, 5460, <https://doi.org/10.1021/es048048q>,  
738 2005.

739 Moset, V., Cambra-López, M., Estellés, F., Torres, A. G., and Cerisuelo, A.: Evolution of  
740 chemical composition and gas emissions from aged pig slurry during outdoor storage with  
741 and without prior solid separation, *Biosyst. Eng.*, 111, 2–10,  
742 <https://doi.org/10.1016/j.biosystemseng.2011.10.001>, 2012.

743 Ngwabie, N. M., Jeppsson, K. H., Gustafsson, G., and Nimmermark, S.: Effects of animal  
744 activity and air temperature on methane and ammonia emissions from a naturally ventilated  
745 building for dairy cows, *Atmos. Environ.*, 45, 6760–6768,  
746 <https://doi.org/10.1016/j.atmosenv.2011.08.027>, 2011.

747 Ngwabie, N.M., Schade, G.W., Custer, T.G., Linke, S., and Hinz, T.: Abundances and flux

748 estimates of volatile organic compounds from a dairy cowshed in Germany, *J. Environ. Qual.*,  
749 37, 565–573, <https://doi.org/10.2134/jeq2006.0417>, 2008.

750 Ni, J. Q., and Heber, A. J.: Sampling and Measurement of Ammonia at Animal Facilities, *Adv.*  
751 *Agron.*, 98, 201–269, [https://doi.org/10.1016/s0065-2113\(08\)00204-6](https://doi.org/10.1016/s0065-2113(08)00204-6), 2008.

752 Ni, J. Q., Diehl, C. A., Chai, L., Chen, Y., Heber, A. J., Lim, T. T., and Bogan, B. W.: Factors  
753 and characteristics of ammonia, hydrogen sulfide, carbon dioxide, and particulate matter  
754 emissions from two manure-belt layer hen houses, *Atmos. Environ.*, 156,  
755 <https://doi.org/10.1016/j.atmosenv.2017.02.033>, 2017.

756 Norman, M., Hansel, A., and Wisthaler, A.: O<sub>2</sub><sup>+</sup> as reagent ion in the PTR-MS instrument:  
757 Detection of gas-phase ammonia, *Int. J. Mass Spectrom.*, 265, 382–387,  
758 <https://doi.org/10.1016/j.ijms.2007.06.010>, 2007.

759 Osada, T., and Fukumoto, Y.: Development of a new dynamic chamber system for measuring  
760 harmful gas emissions from composting livestock waste, *Water Sci. Technol.*, 44, 79–86,  
761 <https://doi.org/10.2166/wst.2001.0513>, 2001.

762 Osada, T., Rom H.B., and Dahl P.: Continuous measurement of nitrous oxide and methane  
763 emission in pig units by infrared photoacoustic detection, *T. ASAE*, 41, 1109–1114,  
764 <https://doi.org/10.13031/2013.17256>, 1998.

765 Paulot, F., Jacob, D. J., Pinder, R. W., Bash, J. O., Travis, K., and Henze, D. K.: Ammonia  
766 emissions in the United States, European Union, and China derived by high - resolution  
767 inversion of ammonium wet deposition data: Interpretation with a new agricultural emissions  
768 inventory (MASAGE\_NH<sub>3</sub>), *J. Geophys. Res.*, 119, 4343–4364,  
769 <https://doi.org/10.1002/2013JD021130>, 2015.

770 Pearson, J., and Stewart, G. R.: The deposition of atmospheric ammonia and its effects on plants,  
771 New Phytol., 125, 283–305, <https://doi.org/10.1111/j.1469-8137.1993.tb03882.x>, 1993.

772 Picarro.: Technology: Cavity Ring-Down Spectroscopy (CRDS), Link:  
773 [https://www.picarro.com/technology/cavity\\_ring\\_down\\_spectroscopy](https://www.picarro.com/technology/cavity_ring_down_spectroscopy). Accessed 12<sup>th</sup> May,  
774 2018.

775 Phillips, V. R., Lee, D. S., Scholtens, R., Garland, J. A., and Sneath, R. W.: SE—Structures and  
776 Environment : A Review of Methods for measuring Emission Rates of Ammonia from  
777 Livestock Buildings and Slurry or Manure Stores, Part 2: monitoring Flux Rates,  
778 Concentrations and Airflow Rates, J. Agr. Eng. Res., 78, 1–14,  
779 <https://doi.org/10.1006/jaer.2000.0618>, 2001.

780 Pinder, R. W., Adams, P. J., and Pandis, S. N.: Ammonia emission controls as a cost-effective  
781 strategy for reducing atmospheric particulate matter in the Eastern United States, Environ.  
782 Sci. Technol., 41, 380–6, <https://doi.org/10.1021/es060379a>, 2007.

783 Rabaud, N.E., Ebeler, S.E., Ashbaugh, L.L., and Flocchini, R.G.: Characterization and  
784 quantification of odorous and non-odorous volatile organic compounds near a commercial  
785 dairy in California, Atmos. Environ., 37, 933–940, [https://doi.org/10.1016/S1352-](https://doi.org/10.1016/S1352-2310(02)00970-6)  
786 [2310\(02\)00970-6](https://doi.org/10.1016/S1352-2310(02)00970-6), 2003.

787 Rong L., Liu D., Pedersen E.F., and Zhang G.: Effect of climate parameters on air exchange  
788 rate and ammonia and methane emissions from a hybrid ventilated dairy cow building, Energ.  
789 Buildings, 82, 632–643, <https://doi.org/10.1016/j.enbuild.2014.07.089>, 2014.

790 Rong L., Liu D., Pedersen E.F., Zhang G. The effect of wind speed and direction and  
791 surrounding maizeon hybrid ventilation in a dairy cow building in Denmark. Energy and

792 Buildings, 86, 25-34, [https://doi.org/ 10.1016/j.enbuild.2014.10.016](https://doi.org/10.1016/j.enbuild.2014.10.016), 2015.

793 Rong, L., Nielsen, P. V., and Zhang, G. Q.: Effects of airflow and liquid temperature on  
794 ammonia mass transfer above an emission surface: experimental study on emission rate,  
795 Bioresource Technol., 100, 4654–4661, <https://doi.org/10.1016/j.biortech.2009.05.003>, 2009.

796 Schilt, S., Thévenaz, L., Niklès, M., Emmenegger, L., and Hüglin, C.: Ammonia monitoring at  
797 trace level using photoacoustic spectroscopy in industrial and environmental applications,  
798 Spectrochim. Acta. A, 60, 3259–3268, <https://doi.org/10.1016/j.saa.2003.11.032>, 2004.

799 Scholtens, R., Jones, C. J. D. M., Lee, D. S., and Phillips, V. R.: Measuring ammonia emission  
800 rates from livestock buildings and manure stores—part 1: development and validation of  
801 external tracer ratio, internal tracer ratio and passive flux sampling methods, Atmos. Environ.,  
802 38, 3003–3015, <https://doi.org/10.1016/j.atmosenv.2004.02.030>, 2004.

803 Seinfeld, J.H.; and Pandis, S.N.: Atmospheric Chemistry and Physics: From Air Pollution to  
804 Climate Change, Wiley-VCH: New York. 1326 pp., ISBN 0-471-17815-2, 1997.

805 Shaw, S.L., Mitloehner, F.M., Jackson, W., Depeters, E.J., Fadel, J.G., Robinson, P.H.,  
806 Holzinger, R., and Goldstein, A.H.: Volatile organic compound emissions from dairy cows  
807 and their waste as measured by proton-transfer-reaction mass spectrometry, Environ. Sci.  
808 Technol., 41, 1310–1316, <https://doi.org/10.1021/es061475e>, 2007.

809 Smith, P., Martino, D., Cai, Z., Gwary, D., Janzen, H., Kumar, P., Mccarl, B., Ogle, S., O'Mara,  
810 F., and Rice, C.: Greenhouse gas mitigation in agriculture, Philos. T. R. Soc. B, 363, 789–  
811 813, <https://doi.org/10.1098/rstb.2007.2184>, 2008.

812 Thomas, C. D., Cameron, A., Green, R. E., Bakkenes, M., Beaumont, L. J., Collingham, Y. C.,  
813 Erasmus, B. F., De Siqueira, M. F., Grainger, A., and Hannah, L.: Extinction risk from climate

814 change, *Nat.*, 427, 145–148, <https://doi.org/10.1038/nature02121>, 2004.

815 Van Breemen, N., Mulder, J., and Driscoll, C. T.: Acidification and alkalization of soils, *Plant*  
816 *Soil*, 75, 283–308, <https://doi.org/10.1007/BF02369968>, 1983.

817 Von Bobrutzki, K., Braban, C.F., Famulari, D., Jones, S.K., Blackall, T., Smith, T.E.L., Blom,  
818 M., Coe, H., Gallagher, M., Ghalaieny, M., McGillen, M.R., Percival, C.J., Whitehead, J.D.,  
819 Ellis, R., Murphy, J., Mohacsi, A., Pogany, A., Junninen, H., Rantanen, S., Sutton, M.A., and  
820 Nemitz, E.: Field inter-comparison of eleven atmospheric ammonia measurement techniques,  
821 *Atmos. Meas. Tech.*, 3, 91–112, <https://doi.org/10.5194/amt-3-91-2010>, 2010.

822 Vries, J. W. D., and Melse, R. W.: Comparing environmental impact of air scrubbers for  
823 ammonia abatement at pig houses: A life cycle assessment, *Biosyst. Eng.*, 161, 53–61,  
824 <https://doi.org/10.1016/j.biosystemseng.2017.06.010>, 2017.

825 Wang-Li L., Li Q.-F., Chai L., Cortus E.L., Wang K., Kilic I., Bogan B.W., Ni J.-Q., and Heber  
826 A.J.: The national air emissions monitoring study's Southeast Layer Site: Part III. Ammonia  
827 concentrations and emissions, *T. ASABE*, 56, 1185–1197, [https://](https://doi.org/10.13031/trans.56.9673)  
828 [doi.org/10.13031/trans.56.9673](https://doi.org/10.13031/trans.56.9673), 2013.

829 Yuan, B., Koss, A.R., Warneke, C., Coggon, M., Sekimoto, K., and de Gouw, J.A.: Proton-  
830 Transfer-Reaction Mass Spectrometry: Applications in Atmospheric Sciences, *Chem. Rev.*,  
831 117, 13187–13229, <https://doi.org/10.1021/acs.chemrev.7b00325>, 2017.

832 Zhao, L., Hadlocon, L. J. S., Manuzon, R. B., Darr, M. J., Keener, H. M., Heber, A. J., and Ni,  
833 J.: Ammonia concentrations and emission rates at a commercial poultry manure composting  
834 facility, *Biosyst. Eng.*, 150, 69–78, <https://doi.org/10.1016/j.biosystemseng.2016.07.006>,  
835 2016.

836 Zhao, Y., Pan, Y., Rutherford, J., and Mitloehner, F. M.: Estimation of the Interference in Multi-  
837 Gas Measurements Using Infrared Photoacoustic Analyzers, *Atmos.*, 3, 246–265,  
838 <https://doi.org/10.3390/atmos3020246>, 2012.